Available online at www.sciencedirect.com
SCIENCE DIRECT
Journal of Catalysis 238 (2006) 353–360
JOURNAL OF CATALYSIS
www.elsevier.com/locate/jcat

Formation of highly concentrated hydrogen through methane decomposition over Pd-based alloy catalysts

Hitoshi Ogihara [a,*,1], Sakae Takenaka [a], Ichiro Yamanaka [a], Eishi Tanabe [b], Akira Genseki [c], Kiyoshi Otsuka [a]

[a] *Department of Applied Chemistry, Graduate School of Science and Engineering, Tokyo Institute of Technology, Ookayama, Meguro-ku, Tokyo 152-8552, Japan*
[b] *Western Hiroshima Prefecture Industrial Institute, Kagamiyama, Higashi-Hiroshima, Hiroshima 739-0046, Japan*
[c] *Center for Advanced Materials Analysis, Tokyo Institute of Technology, Ookayama, Meguro-ku, Tokyo 152-8552, Japan*

Received 15 October 2005; revised 19 December 2005; accepted 22 December 2005

Available online 27 January 2006

Abstract

Highly concentrated hydrogen and carbon nanofibers were produced through methane decomposition in a temperature range of 973–1123 K. Pd-based alloys containing Ni, Co, Rh, or Fe showed high catalytic activity and long life for methane decomposition at 973 K. In particular, Pd–Co/Al_2O_3 and Pd–Ni/Al_2O_3 showed the highest hydrogen yield at reaction temperatures above 973 K among all the catalysts tested. Highly concentrated hydrogen (>94 vol%) was formed by methane decomposition over Pd–Co/Al_2O_3 at 1123 K. SEM images of catalysts [M/Al_2O_3 (M = Fe, Co, Ni, and Pd) and Pd–M/Al_2O_3 (M = Fe, Co, Ni, Cu, Ag, and Rh)] after methane decomposition showed the formation of carbons with fibrous structure. In addition, TEM images of Pd–Co/Al_2O_3 at the initial stage of reaction showed that Pd–Co alloy particles formed carbons from several facets, whereas Co or Pd metal particles formed carbon nanofibers from one facet. This would be one reason why Pd–Co alloy catalysts showed high activity and long life for methane decomposition at high temperatures.

Keywords: Pd-based alloy catalysts; Pure hydrogen; Carbon nanofibers; Pd–Co alloys

1. Introduction

Hydrogen fuel has drawn increasing attention as clean energy in recent years, because it emits no CO_2 when used in H_2–O_2 fuel cells. The current processes for the production of hydrogen (i.e., steam reforming, partial oxidation, and autothermal reforming of methane) inevitably produce a large amount of CO_2 and leave an intolerable amount of CO impurities even after the water–gas shift reaction of CO is performed. CO in hydrogen fuel strongly poisons the anode electrocatalyst in the fuel cells. In addition, if hydrogen produced through these processes is stored in high-pressure cylinders, as many automakers are planning, CO_2 must be cleaned out from hydrogen to avoid the blocking of the cylinder exit by the condensation of CO_2 at the adiabatic expansion of hydrogen when hydrogen is discharged.

Decomposition of methane, as follows, is one of the alternative methods for the hydrogen production [1–3]:

$$CH_4 \rightarrow 2H_2 + C. \quad (1)$$

Methane decomposition produces only hydrogen as a gaseous product. Therefore, hydrogen formed through methane decomposition does not require the elimination of CO or CO_2. Carbons from methane are deposited on the catalysts to grow as carbon nanofibers. Carbon nanofibers are expected to be attractive carbonaceous nanoscale materials [4]. Many uses of carbon nanofibers have been proposed, including electronic components [5], gas storage materials [6], and catalyst supports [7–9]. Therefore, methane decomposition is drawing attention for the production of not only pure hydrogen, but also carbon nanofibers.

For the production of highly concentrated hydrogen through methane decomposition, higher one-pass conversion of methane

* Corresponding author. Fax: +81 11 706 9163.
E-mail address: ogihara@cat.hokudai.ac.jp (H. Ogihara).
[1] Present address: Catalysis Research Center, Hokkaido University, N21-W10 Kita-ku, Sapporo 001-0021, Japan.

0021-9517/$ – see front matter
doi:10.1016/j.jcat.2005.12.024

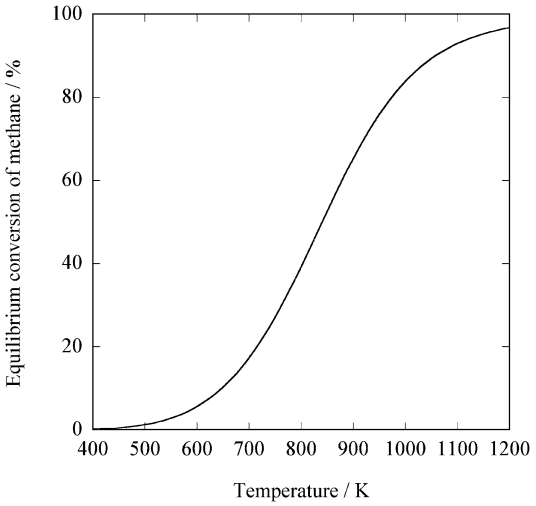

Fig. 1. The equilibrium conversion of methane as a function of the reaction temperature for methane decomposition. Initial composition of the reaction mixture and the pressure are 100% CH_4 and 1 bar, respectively.

is desirable. Fig. 1 shows the equilibrium conversion of methane as a function of the reaction temperature for methane decomposition. The equilibrium conversion of methane was estimated, assuming that carbon formed by methane decomposition was graphite ($CH_4 \leftrightarrow 2H_2 + C$(graphite)). As shown in Fig. 1, methane conversion is not as high when methane decomposition is performed at temperatures below 873 K. It is well known that supported Ni catalysts are effective for methane decomposition in the temperature range of 673–873 K but are deactivated immediately at temperatures above 873 K [3]. Therefore, highly concentrated hydrogen cannot be produced through methane decomposition over Ni catalysts. In contrast, Fe catalysts can decompose methane at a temperature range of 973–1273 K, but Fe catalysts have a very short lifetime [10]. For example, Ermakova et al. reported that Fe catalysts were effective for methane decomposition in the temperature range of 923–1073 K [11]; however, the hydrogen yield (H_2/M: mol of H_2 formed per mol of metals contained in the catalyst) at 1073 K for Fe catalysts (H_2/Fe = 418) was much lower than that at 773 K for Ni catalysts (H_2/Ni = 4802) [3]. Recently, it was reported that Ni–Cu alloy catalysts showed higher activity and longer life for methane decomposition at 948 K than Ni catalysts [12]. The maximum conversion of methane for Ni–Cu alloy catalysts reached ca. 35%. In addition, it was reported that Fe–M (M = Mo, Pd, and Ni) alloy catalysts showed high activities for methane decomposition at 973–1073 K [13]. However, quantitative evaluation of catalytic life was not examined in detail. To supply hydrogen for H_2–O_2 fuel cells directly, it is desirable to attain higher methane conversion and longer catalytic life. We have investigated the improved activity of supported Ni catalysts by addition of other metals, and reported that Pd–Ni alloy catalysts were effective for methane decomposition at 1023 K [14]. In the present study, we found that Pd–Co, Pd–Rh, or Pd–Fe alloy catalysts also showed high activity and long life for methane decomposition above 973 K. The catalytic performance of these Pd-based alloy catalysts is described in detail.

2. Experimental

2.1. Preparation of catalysts

2.1.1. Al_2O_3-supported metal catalysts

Al_2O_3-supported metal catalysts were prepared by impregnating Al_2O_3 (JRC-ALO-8) with an aqueous solution containing the corresponding metal cations. JRC-ALO-8 was supplied as a reference catalyst from the Catalysis Society of Japan. $Co(NO_3)_2{\cdot}6H_2O$, $Fe(NO_3)_3{\cdot}9H_2O$, $Ni(NO_3)_2{\cdot}6H_2O$, and $PdCl_2$ were used as metal precursors. The impregnated samples were dried at 353 K. The dried samples were reduced with hydrogen at 573 K for 1 h and treated under Ar at 923 K for 3 h. The loading of metal in the catalyst was adjusted to be 25 mol%. Al_2O_3-supported metal (M) catalyst is denoted as M/Al_2O_3 hereinafter.

2.1.2. Al_2O_3-supported Pd alloy catalysts

Pd-based alloy catalysts supported on Al_2O_3 were prepared by impregnating Al_2O_3 (JRC-ALO-8) with an aqueous solution containing the corresponding metal cations. $RhCl_3{\cdot}3H_2O$, $Cu(NO_3)_2{\cdot}3H_2O$, $AgNO_3$, and $PdCl_2$ were used as metal precursors. The other precursors were the same as described in Section 2.1.1. Al_2O_3-supported alloys, composed of Pd and foreign metal (M), are denoted as Pd–M/Al_2O_3. The impregnated samples were dried at 353 K. The dried samples were reduced with hydrogen at 573 K for 1 h and treated under Ar at 923 K for 3 h. Only Pd–Fe/Al_2O_3 catalyst was treated under Ar at 773 K for 3 h, because the activity of Pd–Fe/Al_2O_3 was sensitive to the treatment temperature under Ar. For example, Pd–Fe/Al_2O_3 catalysts treated at 923 K under Ar showed lower activity for methane decomposition than that treated at 773 K. The total loading of metals in Pd–M/Al_2O_3 was adjusted to 50 mol%, and the molar ratio of Pd to M in Pd–M/Al_2O_3 catalysts was fixed at 1.0 (i.e., Pd/M = 1.0).

2.2. Methane decomposition

Decomposition of methane was carried out with a conventional gas-flow system at an atmospheric pressure. Before the reaction, the catalyst (0.030 g) was reduced with hydrogen (50.7 kPa) at 573 K for 1 h. Subsequently, the catalyst bed was heated to the reaction temperature under Ar. Decomposition of methane was initiated by contacting methane ($P(CH_4)$ = 101 kPa, flow rate =5–80 ml min^{-1}) with the catalyst. The flow rate was measured at STP. During methane decomposition, a part of exit gas from the catalyst bed was sampled out and analyzed by gas chromatography. The temperature shown in this study was measured outside of the reactor near the catalyst bed.

2.3. Characterization of catalysts

X-ray diffraction (XRD) patterns of the catalyst samples were measured by a Rigaku RINT 2500 V diffractometer using Cu-K_α radiation at room temperature. The scanning rate was 2.0° 2θ/min. Scanning electron microscopy (SEM) images of

carbons deposited on the catalysts by methane decomposition were measured by using a Hitachi FE-SEM S-800 operated at 15 kV. Transmission electron microscopy (TEM) images of carbons deposited on the catalysts by methane decomposition were measured using a JEOL JEM-3000F operated at 200 kV.

3. Results and discussion

3.1. Methane decomposition over M/Al_2O_3 catalysts

Fig. 2 shows changes in methane conversion with time on stream in methane decomposition over M/Al_2O_3 (M = Fe, Co, Ni and Pd) catalysts at 973 K. The product in the gas phase was hydrogen for all catalysts. The conversion of methane was evaluated on the basis of the amount of hydrogen formed according to Eq. (1). The conversion of methane for Fe, Co, and Ni/Al_2O_3 catalysts was very low (<2%) even early in the reactions, and these catalysts were deactivated quickly. In contrast, the catalytic activity of Pd/Al_2O_3 was significantly higher than those of the other catalysts early in the reaction; the initial conversion of methane for Pd/Al_2O_3 catalyst was 15%. However, Pd/Al_2O_3 catalyst was deactivated rapidly with time on stream. At 270 min of time on stream, the methane conversion for Pd/Al_2O_3 was reduced to <1%. Hydrogen yields (H_2/M: mol of H_2 formed per mol of metals contained in the catalyst) after methane decomposition shown in Fig. 2 are given in Table 1.

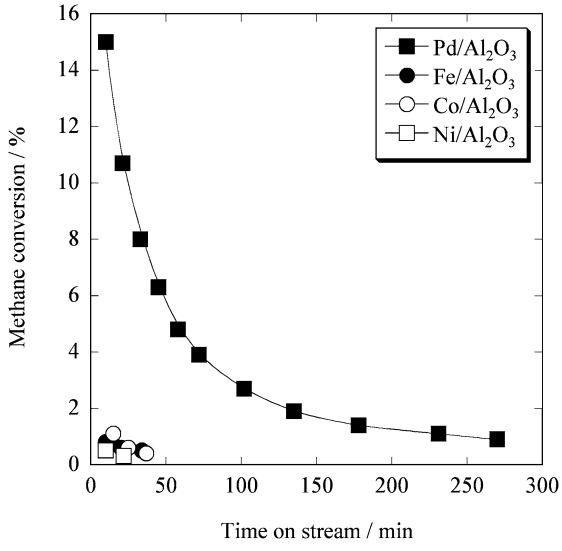

Fig. 2. Kinetic curves of methane conversion in methane decomposition over M/Al_2O_3 (M = Pd, Fe, Co and Ni) at 973 K. Flow rate = 80 ml min^{-1}, amount of catalyst = 0.030 g.

Table 1
Hydrogen yields for M/Al_2O_3 (M = Pd, Ni, Co and Fe) catalysts

Catalysts	Reaction temperature (K)	Hydrogen yields (–)
Pd/Al_2O_3	973	906
Ni/Al_2O_3	973	0.1
Co/Al_2O_3	973	0.3
Fe/Al_2O_3	973	0.3

The hydrogen yield of Pd/Al_2O_3 was extremely high; however, the hydrogen yield of Pd/Al_2O_3 at 973 K ($H_2/Pd = 906$) was much lower than that of Ni/SiO_2 at 773 K ($H_2/Ni = 4802$) [3]. Therefore, for the production of highly concentrated hydrogen through methane decomposition, the activity and life of Pd catalyst should be improved. Recently, it was reported that alloy catalysts such as Ni–Cu alloys or Pd–Ni alloys showed high activity for methane decomposition above 973 K [12–14]. Therefore, we examined the catalytic performance of Pd-based alloy catalysts for methane decomposition in the temperature range of 973–1123 K.

3.2. Methane decomposition over $Pd–M/Al_2O_3$ catalysts

Fig. 3 shows XRD patterns of Pd/Al_2O_3 and $Pd–M/Al_2O_3$ (M = Ni, Co, Rh, Fe, Cu, and Ag) before reaction, as well as the pattern of Ni metal powder as a reference sample. In the XRD pattern of Pd/Al_2O_3, the diffraction lines due to Pd metal crystallites were observed at $2\theta = 40.0°$ (Pd(111)) and 46.5° (Pd(200)), indicating that Pd species in Pd/Al_2O_3 were present as Pd metal crystallites. In the XRD pattern of $Pd–Ni/Al_2O_3$, two diffraction lines at 41.7° and 48.5° were observed, and they were not consistent with those due to Pd metal or Ni metal (spectrum (b)). Diffraction lines for $Pd–Ni/Al_2O_3$ were positioned between those due to Pd metal and those due to Ni metal, indicating the formation of Pd–Ni alloys. Because any diffraction lines due to compounds containing Pd or Ni except for Pd–Ni alloys were not observed in the XRD pattern of $Pd–Ni/Al_2O_3$, most of Pd and Ni species in $Pd–Ni/Al_2O_3$ formed Pd–Ni alloys. XRD patterns of $Pd–Co/Al_2O_3$, $Pd–Rh/Al_2O_3$, $Pd–Fe/Al_2O_3$, $Pd–Cu/Al_2O_3$, and $Pd–Ag/Al_2O_3$ also indicated the formation of the corresponding Pd–M alloys [15–19].

Fig. 4 shows changes in the methane conversion with time on stream for methane decomposition over $Pd–M/Al_2O_3$ (M = Ni, Co, Rh, Fe, Cu, and Ag) and over Pd/Al_2O_3 at 973 K. For all catalysts, methane decomposition proceeded selectively to

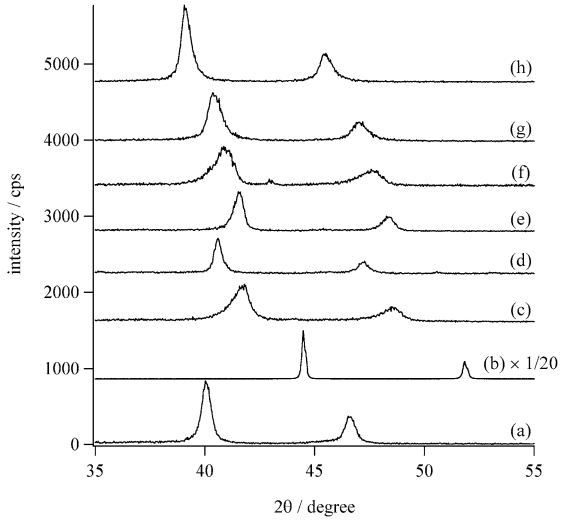

Fig. 3. XRD patterns of Pd/Al_2O_3 and $Pd–M/Al_2O_3$ (M = Ni, Co, Rh, Fe, Cu and Ag) catalysts before methane decomposition, and of Ni powder. (a) Pd/Al_2O_3; (b) Ni metal powder; (c) $Pd–Ni/Al_2O_3$; (d) $Pd–Fe/Al_2O_3$; (e) $Pd–Co/Al_2O_3$; (f) $Pd–Cu/Al_2O_3$; (g) $Pd–Rh/Al_2O_3$; and (h) $Pd–Ag/Al_2O_3$.

form hydrogen only as a gaseous product. The initial methane conversion and life of the catalysts for methane decomposition depended strongly on the type of metal added to Pd/Al_2O_3. The initial methane conversions of Pd–Ni/Al_2O_3, Pd–Rh/Al_2O_3, Pd–Co/Al_2O_3, and Pd–Fe/Al_2O_3 were 35, 30, 29, and 23%, respectively, whereas those of Pd–Cu/Al_2O_3 and Pd–Ag/Al_2O_3 were 18 and 2%, respectively. Comparing Figs. 2 and 4 strongly suggests that the formation of alloys between Pd and Ni, Co, Rh, or Fe caused the improvement of catalytic activity and life of Pd for methane decomposition. Pd–Ni/Al_2O_3 showed the highest conversion and the longest life for methane decomposition at 973 K. In contrast, Pd–Cu/Al_2O_3 and Pd–Ag/Al_2O_3 were deactivated quickly. The hydrogen yields for Pd–M/Al_2O_3 are given in Table 2. The hydrogen yields were estimated based on the results shown in Figs. 2 and 4. Pd–Ni/Al_2O_3, Pd–Co/Al_2O_3, Pd–Rh/Al_2O_3, and Pd–Fe/Al_2O_3 showed higher hydrogen yields than Pd/Al_2O_3 ($H_2/Pd = 906$). In particular, the hydrogen yield for Pd–Ni/Al_2O_3 was 20 times as high as that for Pd/Al_2O_3. It should be noted that hydrogen yield for Pd–Ni/Al_2O_3 ($H_2/(Pd + Ni) = 20597$) was appreciably larger than the sum of hydrogen yields for Pd/Al_2O_3 ($H_2/Pd = 906$) and for Ni/Al_2O_3 ($H_2/Ni = 0.1$). These results strongly suggest that the activity of Pd catalyst for methane decomposition is improved by the formation of Pd–Ni alloys. As shown in Table 2, Pd–Ni/Al_2O_3, Pd–Co/Al_2O_3, Pd–Rh/Al_2O_3, and Pd–Fe/Al_2O_3 were effective catalysts for methane decomposition at 973 K. Therefore, to increase the methane conversion, methane decomposition was performed over these catalysts at temperatures above 973 K. Fig. 5 shows changes in methane conversion with time on stream for methane decomposition over Pd–M/Al_2O_3 (M = Ni, Co, Rh, and Fe) at 1073 (A) and 1123 K (B). Initial methane conversions for all the catalysts at 1073 K were higher than those at 973 K shown in Fig. 4; however, further improvement of the initial conversion was not caused by increase in the reaction temperature from 1073 to 1123 K. Methane conversions at the early period of reaction for Pd–Ni/Al_2O_3, Pd–Co/Al_2O_3, and Pd–Rh/Al_2O_3 at 1073 K were similar to one another. The order of the catalytic life at temperatures >1073 K was Pd–Co/Al_2O_3 > Pd–Ni/Al_2O_3 ≈ Pd–Rh/Al_2O_3 > Pd–Fe/Al_2O_3, whereas that at 973 K was Pd–Ni/Al_2O_3 > Pd–Co/Al_2O_3 > Pd–Rh/Al_2O_3 > Pd–Fe/Al_2O_3. These results indicate that Pd–Co/Al_2O_3 catalyst is most preferable for methane decomposition at temperatures above 1073 K. Fig. 6 and Table 2 show hydrogen yields for methane decomposition over Pd–Ni/Al_2O_3, Pd–Co/Al_2O_3, Pd–Rh/Al_2O_3, and Pd–Fe/Al_2O_3 at different temperatures. The hydrogen yields were estimated based on the results shown in Figs. 4 and 5. The hydrogen yield for Pd–Ni/Al_2O_3 decreased drastically when the reaction temperature increased from 973 to 1073 K. In contrast, the hydrogen yields for Pd–Co/Al_2O_3 and Pd–Rh/Al_2O_3 decreased moderately when the temperature increased from 973 to 1073 K. In particular, Pd–Co/Al_2O_3 showed the highest hy-

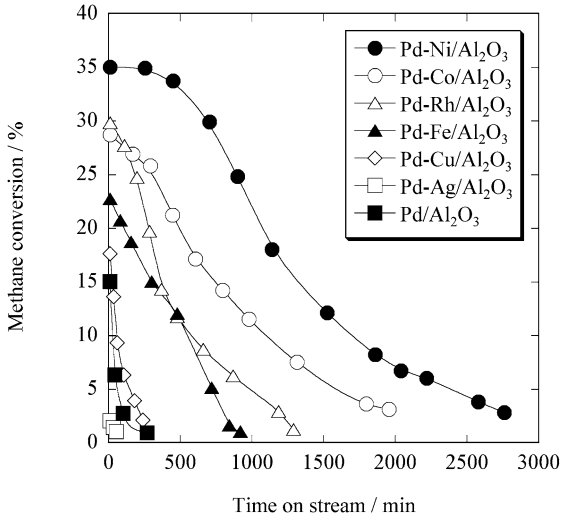

Fig. 4. Kinetic curves of methane conversion in methane decomposition over Pd/Al_2O_3 and Pd–M/Al_2O_3 (M = Ni, Co, Rh, Fe, Cu and Ag) at 973 K. Flow rate = 80 ml min^{-1}, amount of catalyst = 0.030 g.

Table 2
Hydrogen yields for Pd–M/Al_2O_3 (M = Ni, Co, Rh, Fe, Cu and Ag) catalysts

Catalysts	Reaction temperature (K)	Hydrogen yields (–)
Pd–Ni/Al_2O_3	973	20597
	1073	3198
	1123	878
Pd–Co/Al_2O_3	973	10626
	1073	7976
	1123	2051
Pd–Rh/Al_2O_3	973	6268
	1073	3990
	1123	1384
Pd–Fe/Al_2O_3	973	4476
	1073	418
	1123	28
Pd–Cu/Al_2O_3	973	544
Pd–Ag/Al_2O_3	973	38

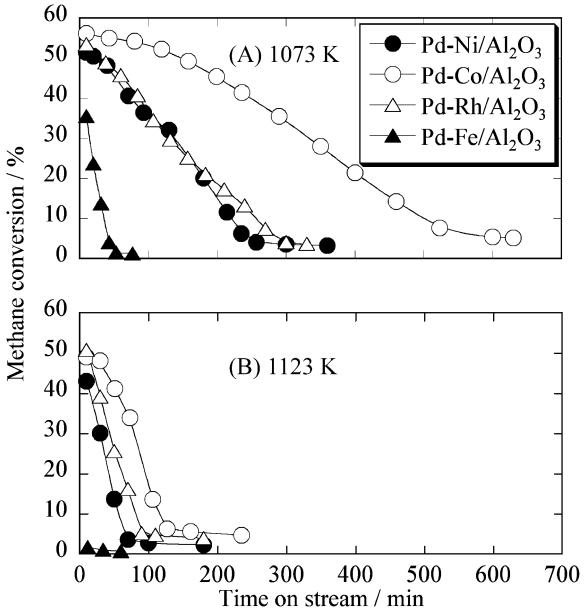

Fig. 5. Kinetic curves of methane conversion in methane decomposition over Pd–M/Al_2O_3 (M = Ni, Co, Rh and Fe) at 1073 K (A) and 1123 K (B). Flow rate = 80 ml min^{-1}, amount of catalyst = 0.030 g.

drogen yield for methane decomposition at temperatures above 1073 K.

To produce highly concentrated hydrogen, methane decomposition was performed over Pd–Co/Al_2O_3 catalysts at 1123 K with high W/F value (W, weight of catalyst; F, flow rate of methane). Fig. 7 shows the methane conversion as a function of time on stream over Pd–Co/Al_2O_3 at 1123 K. Reaction conditions were as follows: amount of catalyst, 0.050 g; $P(CH_4) =$ 101 kPa; reaction temperature 1123 K. The methane flow rate was adjusted to 10 ml min^{-1} in the range of 0–40 min of time on stream. The conversion of methane at 20 min of time on stream was 91.2%. To estimate the equilibrium conversion of methane over Pd–Co/Al_2O_3, the flow rate of methane was decreased from 10 to 5 ml min^{-1} after 40 min time on stream. Although the flow rate of methane decreased from 10 to 5 ml min^{-1}, methane conversion at 60 min remained at 91.2%. This result suggests that the equilibrium conversion of methane at 1123 K over Pd–Co/Al_2O_3 catalysts is ca. 91%. Calculated equilibrium methane conversion at 1123 K is 94% (shown as a dashed line in Fig. 7). The equilibrium conversion of methane was estimated, assuming that carbon formed by methane decomposition was graphite ($CH_4 \leftrightarrow 2H_2 + C$(graphite)), but carbons formed through methane decomposition consist of graphite and amorphous carbons [3]. The presence of amorphous carbon is thought to induce the slight difference between calculated equilibrium conversion and measured equilibrium conversion. Note that methane conversion >90% was constant for 110 min, as shown in Fig. 7, indicating that Pd–Co/Al_2O_3 can produce highly concentrated hydrogen >94 vol% constantly through methane decomposition.

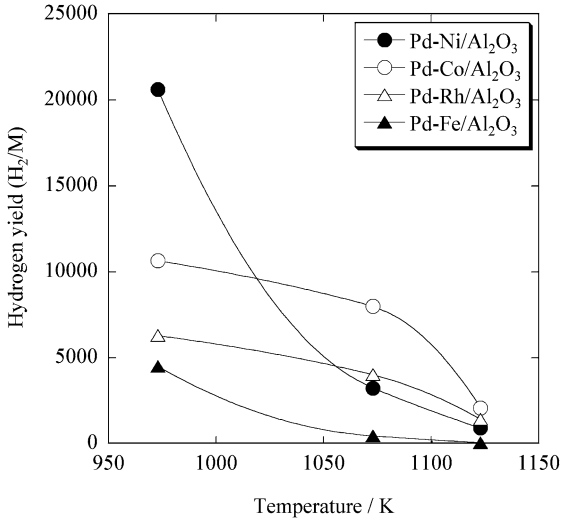

Fig. 6. Changes in the hydrogen yields for Pd–M/Al_2O_3 (M = Ni, Co, Rh and Fe) catalysts as a function of reaction temperatures.

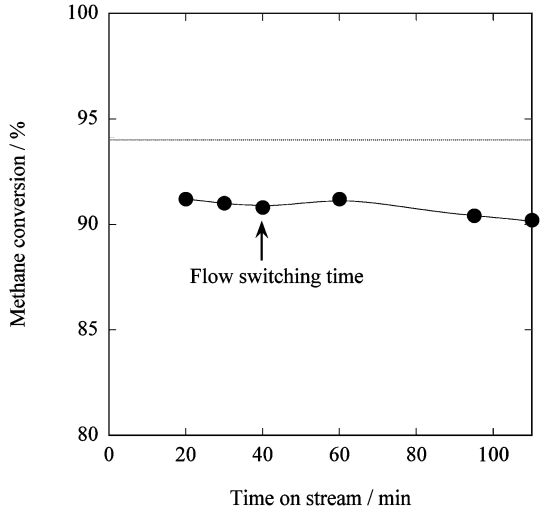

Fig. 7. Methane conversion as a function of time-on-stream over Pd–Co/Al_2O_3 catalysts at 1123 K. Flow rate = 10 ml min^{-1} from 0 to 40 min; 5 ml min^{-1} after 40 min, amount of catalyst = 0.050 g. Dashed line indicates the equilibrium methane conversion at 1123 K.

3.3. SEM and TEM images of the catalysts after methane decomposition

Fig. 8 shows SEM images of M/Al_2O_3 catalysts (M = Pd, Co, Fe, and Ni) after deactivation for methane decomposition at 973 K. In Section 3.3, the catalysts after deactivation refer to the catalysts after methane decomposition shown in Figs. 2, 4 and 5. All of the SEM images showed formation of fibrous carbons on the catalysts. The diameter of fibrous carbons on Co/Al_2O_3, Fe/Al_2O_3, and Ni/Al_2O_3 was several tens of nanometers, whereas that on Pd/Al_2O_3 was significantly larger

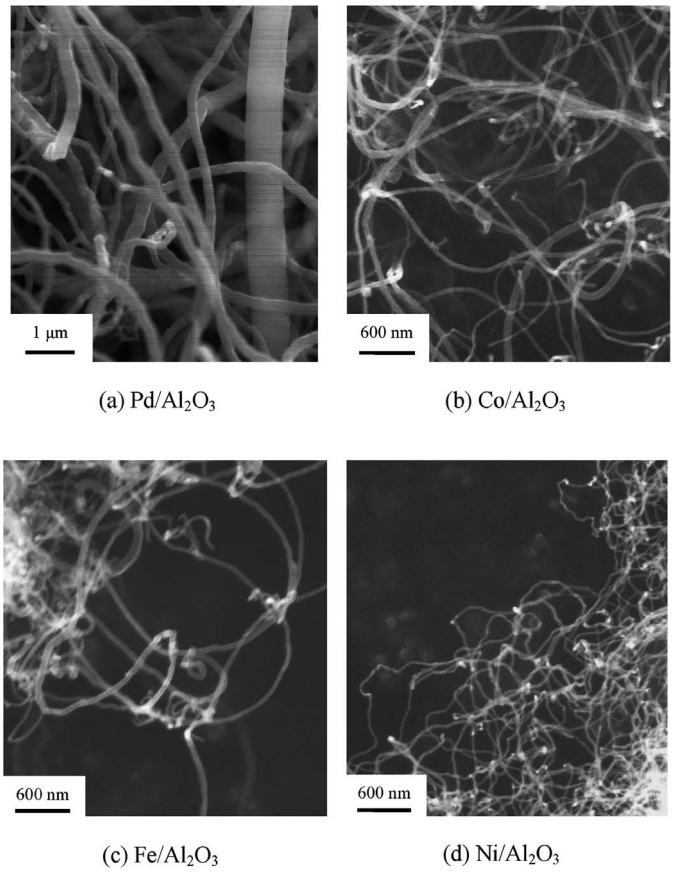

Fig. 8. SEM images of M/Al_2O_3 (M = Pd, Fe, Co and Ni) catalysts after deactivation for methane decomposition at 973 K.

than those on Co/Al_2O_3, Fe/Al_2O_3, and Ni/Al_2O_3. The diameter of carbon nanofibers formed on Pd/Al_2O_3 ranged from 100 to 500 nm. The shapes of carbons shown in Fig. 8 were similar to one another. The generally accepted mechanism for methane decomposition over metal catalysts is as follows. Metal particles decompose methane molecules into hydrogen molecules and carbon atoms. The carbon atoms present on the surface of metal particles diffuse in the body of metal particles and are precipitated from another facet of the metal particles to grow carbon nanofibers. During the reaction, metal particles are present at the tip of carbon nanofibers [4].

Fig. 9 shows SEM images of $Pd–M/Al_2O_3$ catalysts (M = Ni, Co, Rh, and Fe) after deactivation for methane decomposition at 973 K. The shapes of carbons formed on $Pd–Ni/Al_2O_3$, $Pd–Co/Al_2O_3$, $Pd–Rh/Al_2O_3$, and $Pd–Fe/Al_2O_3$ were similar to one another. Carbon nanofibers with a diameter in the range of several tens to several hundreds nanometers were formed over all of the catalysts. Fig. 10 shows SEM images of $Pd–M/Al_2O_3$ (M = Cu and Ag) catalysts after deactivation for methane decomposition at 973 K. As mentioned earlier, $Pd–M/Al_2O_3$ (M = Cu and Ag) catalysts were ineffective for methane decomposition at 973 K. For $Pd–Cu/Al_2O_3$, diameter of formed carbon nanofibers was <50 nm (Fig. 10a). The diameter of carbons deposited on $Pd–Cu/Al_2O_3$ was different from that on the other Pd alloys shown in Fig. 9, indicating that the mechanism of methane decomposition over Pd–Cu alloy is quite different from those over Pd–Ni, Pd–Co, Pd–Rh, and Pd–Fe alloys. For $Pd–Ag/Al_2O_3$, the formation of carbon nanofibers was confirmed, but their length seemed remarkably short (Fig. 10b). The SEM images of $Pd–Ag/Al_2O_3$ implied that Pd–Ag alloys could precipitate carbons as carbon nanofibers at the initial stage of methane decomposition, but Pd–Ag alloys were immediately deactivated by some reasons. Kapinski [20] reported the formation of carbon nanofibers over Pd/CeO_2 through acetylene decomposition. The growth of carbon nanofibers was inhibited by the formation of Pd–Ce alloys when Pd/CeO_2 catalysts were reduced with hydrogen at high temperatures (>1100 K) [20]. The rate of carbon diffusion in the body of Pd–Ce alloy would be slow, so that the deposition rate of carbons on the surface of Pd–Ce alloy particles should overcome the diffusion rate of carbons in the body of Pd–Ce alloys, which brought about the coverage of metal surface with the deposited carbons. This resulted in the rapid deactivation of Pd–Ce alloys for the formation of carbon nanofibers. In the present study, the rate of carbon diffusion in Pd–Ag alloys is likely slow. In contrast, Pd–Ni, Pd–Co, Pd–Rh, and Pd–Fe alloys might rapidly precipitate carbons as graphite during methane decomposition. Therefore, these catalysts would show high activity and long life for methane decomposition.

When alloys are used as catalysts for any catalytic reactions, the atomic fraction of the alloy surface controls the catalytic performance. In the case of Pd–Ag and Pd–Cu alloys, Ag or Cu atoms segregate at the surface of alloy particles [21]. Ag and Cu atoms cannot decompose methane molecules into hydrogen molecules and carbon atoms. This would be one reason why $Pd–Ag/Al_2O_3$ and $Pd–Cu/Al_2O_3$ showed poor activity for methane decomposition. In contrast, in the case of Pd–Ni, Pd–Co, Pd–Rh, and Pd–Fe alloys, Pd atoms segregate at the surface of alloy particles [21–24]. The segregation of Pd atoms on the alloy particles would not inhibit methane decomposition, because Pd atoms can decompose methane into hydrogen molecules and carbon atoms, as shown in the present study.

Pd–Co alloy catalysts showed high activity and long life for methane decomposition at reaction temperatures above 1073 K, as shown in Figs. 5 and 6. Therefore, Pd–Co alloy catalysts and carbons formed over them were investigated. Fig. 11 shows SEM images of $Pd–Co/Al_2O_3$ catalysts after deactivation (a) and at the initial stage of reaction (b) ($H_2/M = 200$) at 1073 K. SEM image (a) showed that the carbons present on the deactivated catalysts had a fibrous structure and ranged in diameter

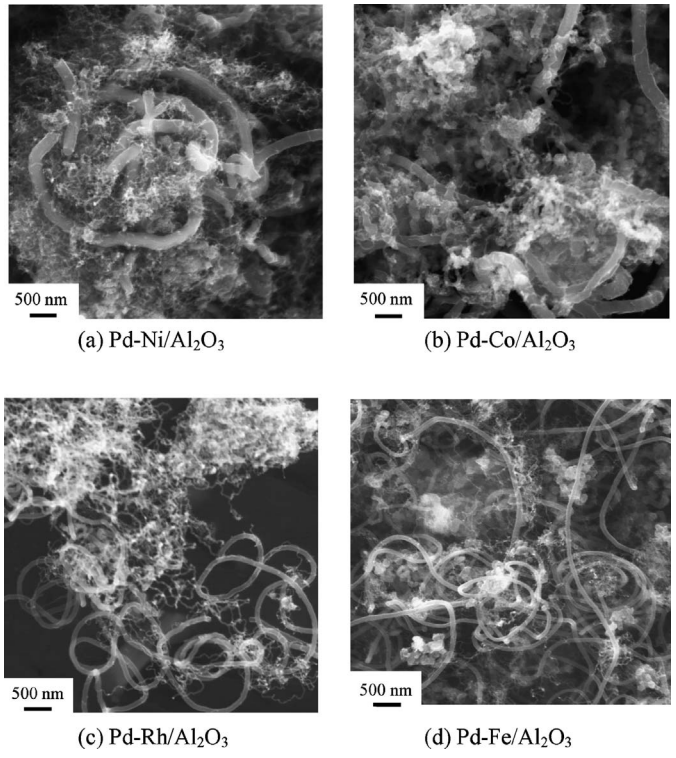

(a) $Pd-Ni/Al_2O_3$ (b) $Pd-Co/Al_2O_3$

(c) $Pd-Rh/Al_2O_3$ (d) $Pd-Fe/Al_2O_3$

Fig. 9. SEM images of $Pd–M/Al_2O_3$ (M = Ni, Co Rh and Fe) catalysts after deactivation for methane decomposition at 973 K.

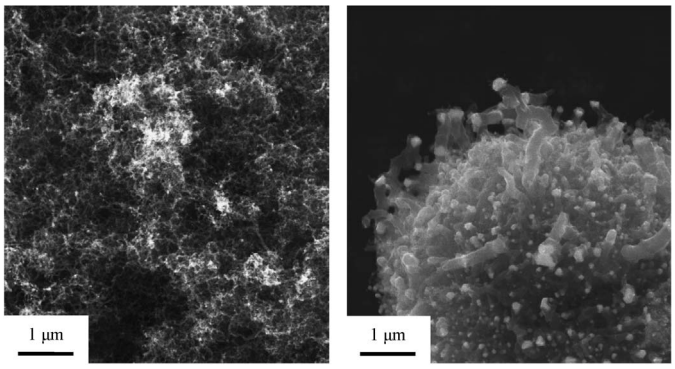

(a) $Pd-Cu/Al_2O_3$ (b) $Pd-Ag/Al_2O_3$

Fig. 10. SEM images of $Pd–M/Al_2O_3$ (M = Cu and Ag) catalysts after deactivation for methane decomposition at 973 K.

from several tens to several hundreds of nanometers. In contrast, the shapes of carbons formed at the initial stage of reaction (Fig. 11b) were quite different from those at the deactivation stage (Fig. 11a). At the initial stage of reaction, Pd–Co alloy catalysts formed carbons without fibrous structure. To investigate the structure of formed carbons and Pd–Co alloys in detail, TEM images of catalysts were measured. Fig. 12 shows a TEM image of Pd–Co/Al_2O_3 catalysts at the initial stage of reaction at 1073 K. Energy-dispersive spectra (EDS) for some darker spots in TEM images were measured at the same time as the TEM images. The EDS showed that the darker spots were composed of Pd and Co atoms, and the molar ratio of Pd/(Pd + Co) was estimated as ca. 0.5. This value was consistent with the molar ratio adjusted at the preparation stage of Pd–Co/Al_2O_3 catalysts. Pd–Co alloy particles with a particle size in the range of 10–100 nm as well as a large amount of deposited carbons are shown in Fig. 12. The shape of carbons formed did not exhibit a clearly fibrous structure. It seems that Pd–Co alloy particles deposited carbons from several facets. As mentioned earlier, in the general mechanism for methane decomposition over metal catalysts such as Ni and Co metal, metal particles grow carbon nanofibers from one facet.

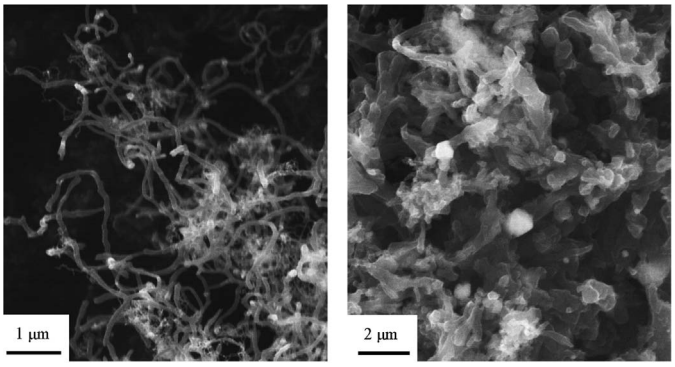

Fig. 11. SEM images of Pd–Co/Al_2O_3 catalysts (a) after deactivation, and (b) at the initial stage of reaction (H_2/M =200) at 1073 K.

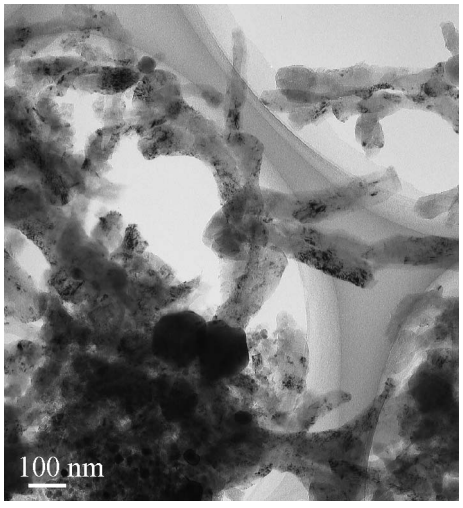

Fig. 12. TEM images of Pd–Co/Al_2O_3 catalysts at the initial stage of methane decomposition (H_2/M = 200) at 1073 K.

During methane decomposition, carbon atoms formed on the catalyst surfaces diffuse in the body of catalyst particles and were precipitated as graphite. Because methane decomposition is performed at higher temperatures, the deposition rate of carbon atoms from methane on the metal surfaces must be higher. If the deposition rate of carbon atoms from methane were to overcome the atoms' diffusion or precipitation rate, then the catalyst surfaces would be covered with deposited carbons, which would cause the deactivation of catalysts for methane decomposition. As shown in Fig. 12, Pd–Co alloy particles precipitated carbons from several facets, whereas metal particles such as Ni and Co metals precipitated carbons from a single facet to form carbon nanofibers. The precipitation rate of carbons for Pd–Co alloys would be higher than that for Co and Ni metals, because the alloys could precipitate carbons from several facets. Thus, the surfaces of Pd–Co alloys would not be covered with deposited carbons during methane decomposition at higher temperatures. This would be one reason why Pd–Co alloy catalysts showed high activity and long life for methane decomposition at high temperatures.

As described earlier, Pd–Co alloy particles formed carbon nanofibers at the deactivation stage of methane decomposition, whereas the alloys formed carbons without fibrous structures at early stages of methane decomposition. This result implies that Pd–Co alloy particles precipitated carbons from one facet of the particles to form carbon nanofibers at the deactivation stage of Pd–Co/Al_2O_3, whereas the alloy particles precipitated carbons from several facets at early stages. The area of the facets that could precipitate carbon atoms would decrease during methane decomposition over Pd–Co/Al_2O_3. Thus, the precipitation rate of carbons from Pd–Co alloy particles should decrease with time on stream, resulting in the deactivation of Pd–Co alloys for methane decomposition.

4. Conclusions

From the findings of this study, we can draw the following conclusions:

1. Pd alloy catalysts showed high activity and long life for methane decomposition at reaction temperatures above 973 K. In particular, Pd–Ni/Al_2O_3 and Pd–Co/Al_2O_3 showed the highest hydrogen yield among all of the catalysts tested. Hydrogen of 94 vol% was formed constantly through methane decomposition over Pd–Co/Al_2O_3 catalyst at 1123 K.
2. Pd–Co alloy particles precipitated carbon atoms from several facets, whereas Pd or Co metal formed carbon nanofibers from one facet.

References

[1] T.V. Choudhary, C. Sivadinarayana, C.C. Chusuei, A. Klinghoffer, D.W. Goodman, J. Catal. 199 (2001) 9.
[2] T. Ishihara, Y. Miyashita, H. Iseda, Y. Takita, Chem. Lett. 93 (1995).
[3] S. Takenaka, S. Kobayashi, H. Ogihara, K. Otsuka, J. Catal. 217 (2003) 79.
[4] K.P. de Jong, J.W. Geus, Catal. Rev. Sci. Eng. 42 (2000) 481.

[5] C. Niu, E.K. Sichel, R. Hoch, D. Moy, H. Tennent, Appl. Phys. Lett. 70 (1997) 1480.
[6] G.E. Gadd, M. Blackford, S. Moricca, N. Webb, P.J. Evans, A.M. Smith, G. Jacobsen, S. Leung, A. Day, Q. Hua, Science 277 (1997) 933.
[7] R. Gao, C.D. Tan, R.T.K. Baker, Catal. Today 65 (2001) 19.
[8] A. Chambers, T. Nemes, N.M. Rodriguez, R.T.K. Baker, J. Phys. Chem. B 102 (1998) 2251.
[9] K. Otsuka, H. Ogihara, S. Takenaka, Carbon 41 (2003) 223.
[10] S. Takenaka, M. Serizawa, K. Otsuka, J. Catal. 222 (2004) 520.
[11] M.A. Ermakova, D.Y. Ermakov, A.L. Chuvilin, G.G. Kuvshinov, J. Catal. 201 (2001) 183.
[12] T.V. Reshetenko, L.B. Avdeeva, Z.R. Ismagilov, A.L. Chuvilin, V.A. Ushakov, Appl. Catal. A 247 (2003) 51.
[13] N. Shaha, D. Panjala, G.P. Huffman, Energy Fuels 15 (2001) 1528.
[14] S. Takenaka, Y. Shigeta, E. Tanabe, K. Otsuka, J. Catal. 220 (2003) 468.
[15] F.B. Noronha, M. Schmal, B. Moraweck, P. Delichère, M. Brun, F. Villain, R. Fréty, J. Phys. Chem. B 104 (2000) 5478.
[16] G.W. Graham, H. Sun, H.-W. Jen, X.Q. Pan, R.W. McCabe, Catal. Lett. 81 (2002) 1.
[17] F. Pinna, M. Selva, M. Signoretto, G. Strukul, F. Boccuzzi, A. Benedetti, P. Canton, G. Fagherazzi, J. Catal. 150 (1994) 356.
[18] J. Batista, A. Pintar, J.P. Gomilek, A. Kodre, F. Bornette, Appl. Catal. A 217 (2001) 55.
[19] C. Damle, A. Kumar, M. Sastry, J. Phys. Chem. B 106 (2002) 297.
[20] L. Kapinski, Catal. Today 50 (1999) 237.
[21] J.L. Rousset, J.C. Bertolini, P. Miegge, Phys. Rev. B 53 (1996) 4947.
[22] T. Maillet, J. Barbier Jr., P. Gelin, H. Praliaud, D. Duprez, J. Catal. 202 (2001) 367.
[23] P.J. Godowski, S.M. Zuber, J. Mater. Chem. 9 (1999) 1835.
[24] J.C. Bertolini, Y. Debauge, P. Delichere, J. Massardier, J.L. Rousset, P. Ruiz, B. Tardy, Stud. Surf. Sci. Catal. 75 (1993) 1751.